Characteristic parameters of nonlinear surface envelope waves beneath an ice cover under pre-stress

Andrej T. Il'ichev[1,2], Viktor Ja. Tomashpolskii[2]

[1] Steklov Mathematical Institute, Gubkina str. 8, 119991 Moscow, Russia

[2] Bauman Moscow Technical University, Baumanskaya str. 5, 105110 Moscow, Russia

February 9, 2019

Dedicated to the memory of A.M. Samsonov

Abstract

In this paper we focus our attention on physical parameters of so-called envelope solitary waves beneath an ice cover. The form and propagation of waves in water basins under the ice cover are described by the 2D Euler equations. The ice cover is modeled by an elastic Kirchhoff-Love plate and is assumed to be of considerable thickness so that the inertia of the plate is taken into account in the formulation of the model. The Euler equations involve the additional pressure from the plate that freely floats at the surface of the fluid. We consider both the self-focusing case, when envelope solitary waves exist, for which the envelope speed (group speed) is equal to the velocity of filling (phase velocity) and the defocusing case, when they are replaced by so-called dark solitons. The indicated families of waves are parameterized by the velocity of the waves, and their existence is proved earlier for velocities lying in some neighbourhood of the critical value corresponding to the quiescent state. The waves, in turn, bifurcate from the quiescent state and lie in some neighbourhood of it. Analysing the critical parameters for above mentioned waves we determine characteristic values of the length and velocity of the wave. These physical parameters can be compared with possible observations detecting such waves in practice.

1 INTRODUCTION

Both envelope solitary waves and dark solitons correspond to solutions of traveling wave type of the full 2D Euler equations of an ideal incompressible fluid in the presence of the ice cover. Geometrically nonlinear model of the ice based on Kirchhoff-Love plate theory was **first** used in [1, 2] for a certain periodic flexural-gravity wave problem. Combination of the normal form theory described in [3] with the centre manifold reduction in the spirit of [4] and [5] for water-ice problem where the ice cover was modelled by Kirchhoff-Love's

plate under initial stress for the water of finite depth has been adopted in [6]. The method described in [6] was generalized to the case of a moving load on the ice cover in [7]. The resulting wave structures were compared with numerical solutions. The forced problem of waves on the surface of the fluid of infinite depth under the Kirchhoff-Love elastic plate was studied in [8] with asymptotic and numerical methods. It was shown, in particular, that envelope solitary waves exist only at finite amplitude. Further results on periodic waves, generalized solitary waves and three dimensional waves due to a steadily moving load were obtained in [9, 10]. The possible bifurcations from the quiescent state, when inertia of the Kirchhoff-Love ice plate was taken into consideration was discussed in [11]. It was shown in [6, 7] that for the fluid of finite depth the focusing region was replaced by the defocusing one, namely envelope solitary waves bifurcating from the minimal speed of dispersion relation are replaced by dark solitons, which occurs due to the fact that the coefficient at the leading nonlinearity in the governing equation changes sign. Some examples of the critical depth depending on the ice thickness for free waves were given in [12]. The case when the Kirchhoff-Love ice plate is subjected to the compression was discussed in [13].

For longitudinal strains and stresses in the model of Kirchhoff-Love plate the terms of order $O(h^2/R_m^2)$, where h is the plate thickness and R_m is the curvature radius of the neutral plane of the plate are neglected (see, e. g. [6]). Therefore, the resulting elastic energy of Kirchhoff-Love plate has the corresponding order in h/R_m and the total energy (fluid plus ice) is conserved to a certain order in h/R_m, but is not conserved exactly. In [14] a nonlinear formulation based on the special Cosserat theory theory for hyperelastic shells was proposed which possesses the elastic energy corresponding to exactly conserved total energy. However, experiments show that under natural conditions the ice cover quite often behaves like a thin elastic plate [15].

In [16] the 2D problem of traveling waves propagating at the water-ice interface in the ideal fluid of infinite depth was concerned. The ice cover was modelled as a Cosserat shell via formulation of [14]. In particular, it was shown that no envelope solitary waves exist for small amplitude waves, for larger amplitudes both forced and free steady waves were computed by direct numerical simulations. Branches of two dimensional flexural-gravity waves of finite amplitude via the Cosserat framework were computed numerically in [17]. In [18] the same formulation is presented for the fluid layer of finite depth. As in [6, 7] for Kirchhoff-Love's plate it was shown that there is a critical depth below which the nonlinear Shrödinger equation asymptotically describing waves of small amplitude is of the focusing type and hence admits envelope solitary wave solutions. It was also observed numerically that envelope solitary waves of arbitrary amplitude are stable once they are waves of depression. Solitary, envelope solitary and generalized solitary waves of a two fluid problem either when the Cosserat elastic shell is on the top of the first layer or between two fluids were computed in [19, 20]. The work [21] is concerned with flexural-gravity solitary waves on water of finite depth where the elastic sheet is modelled basing on the Cosserat theory of hyperelastic shells. Both steady and unsteady waves are computed numerically for the full Euler equations by using a conformal mapping technique. Solitary flexural-gravity waves in three dimensions are discussed in [22]. Experimental data concerning ice

waves can be found in [23, 24, 25].

According to the experimental results of [15] the ice cover is modelled here with the help of Kirchhoff-Love's plate. We focus our attention on physical parameters of envelope solitary waves beneath the ice cover. As it was mentioned, here for each value of ice thickness there exist some critical values of water depth and velocity where envelope solitary waves cease to exist, and they are replaced by dark solitons. Hence, there exist a finite range of values of water depth (for fixed value of the ice cover thickness) where a family of envelope solitary waves locally exist (this family may be continued with respect to the wave amplitude). Analysing the form of the envelope solitary wave from this range and the critical parameters for it we determine characteristic values of the length and velocity of the wave in order to compare them with experimental data on detecting free envelope solitary waves beneath the ice. For each value of the ice cover thickness, water depth **and initial pre-stress in the ice cover** we find the corresponding values of wave length, velocity and frequency.

The paper is organized as follows. In Sec. 2 we give the brief formulation of the problem, in Sec. 3 we present the equations in the operator form for traveling waves, their asymptotic form and describe bifurcations leading to their occurrence. In Sec. 4 we briefly describe the centre manifold reduction and approximation of the flow in the centre manifold by the equations in normal form. Sec. 5 is devoted to results of the paper. In Sec. 6 we discuss the results.

2 Formulation

2.1 Model of the ice cover

The equation of the balance of forces acting from the plate to the fluid is reduced to the form [6]:

$$p = p_0 + \frac{\sigma_0 h}{R_m} - \partial_{xx}^2 M + \rho_s h \frac{\partial^2 \eta}{\partial t^2}, \quad M = \frac{J}{R_m}, \quad J = \frac{E h^3}{12(1-\nu^2)}. \tag{2.1}$$

The curvature of a middle surface which is identified with the plate after averaging procedure with respect to plate thickness is given by [1]:

$$\frac{1}{R_m} = -\frac{\partial_{xx}\eta}{(1+(\partial_x \eta)^2)^{3/2} - h\partial_{xx}\eta/2}.$$

The notations for the dimensional physical values and fundamental constants are given in Table 1.

2.2 Equations of the fluid-ice system

We study plane potential motions of the ideal incompressible fluid of finite depth with a horizontal bottom.

Symbol	Value	Dimension
p	pressure in the fluid	$[\mathrm{ML}^{-1}\mathrm{T}^{-2}]$
p_0	atmospheric pressure	$[\mathrm{ML}^{-1}\mathrm{T}^{-2}]$
φ	velocity potential	$[\mathrm{L}^2\mathrm{T}^{-1}]$
η	surface deviation of the ice-fluid interface	$[\mathrm{L}]$
R_m	radius of the middle surface of the plate	$[\mathrm{L}]$
x	horizontal coordinate	$[\mathrm{L}]$
z	vertical coordinate	$[\mathrm{L}]$
h	ice thickness	$[\mathrm{L}]$
H	fluid depth	$[\mathrm{L}]$
g	gravity acceleration	$[\mathrm{LT}^{-2}]$
k	wave number	$[\mathrm{L}^{-1}]$
ω	frequency	$[\mathrm{T}^{-1}]$
σ_0	pre-stress in the plate	$[\mathrm{ML}^{-1}\mathrm{T}^{-2}]$
E	Young module	$[\mathrm{ML}^{-1}\mathrm{T}^{-2}]$
ν	Poisson coefficient	$[\ ]$
ρ	fluid density	$[\mathrm{ML}^{-3}]$
ρ_s	ice density	$[\mathrm{ML}^{-3}]$

Table 1: Notations of the dimensional physical values and fundamental constants.

The fluid occupies the domain

$$D = \{x \in \mathbb{R};\ 0 < z < H + \eta(x)\},$$

with the boundary

$$\partial D = \partial D^+ \cup \partial D^- = \{x \in \mathbb{R}; z = H + \eta(x) \cup z = 0\}.$$

The interface between the fluid and ice is given by the equation $z = H + \eta(x)$, $x \in \mathbb{R}$.

From (2.1) it follows that the Euler equations of the ideal incompressible fluid of finite depth with a horizontal bottom in presence of the mentioned surface effects has the form [6]

$$\begin{aligned}
&\varphi_{xx} + \varphi_{zz} = 0, \quad (x,z) \in D,\\
&\varphi_z = 0, \quad (x,z) \in \partial D^-,\\
&\varphi_t + \frac{1}{2}(\varphi_x^2 + \varphi_z^2) + g\eta - \hat{b}\hat{\kappa}_1 + \frac{J}{\rho}\hat{\kappa}_2 + \hat{c}\eta_{tt} = 0, \quad (x,z) \in \partial D^+,\\
&\eta_t + \eta_x\varphi_x = \varphi_z, \quad (x,z) \in \partial D^+,
\end{aligned} \tag{2.2}$$

where

$$\hat{b} = \frac{h\sigma_0}{\rho}, \quad \hat{c} = \rho_s h/\rho, \quad \hat{\kappa}_1 = \frac{\eta_{xx}}{(1+\eta_x^2)^{3/2} - h\eta_{xx}}, \quad \hat{\kappa}_2 = \partial_{xx}^2 \frac{\eta_{xx}}{(1+\eta_x^2)^{3/2} - h\eta_{xx}}.$$

The letter subscripts denote differentiation with respect to corresponding variables.

The dispersion relation for the system (2.2) has the form

$$\omega^2 = \left[\frac{k\,\mathrm{th}(kH)}{1+\hat{c}k\,\mathrm{th}(kH)}\right]\left[g+\hat{b}k^2+\frac{J}{\rho}k^4\right]. \tag{2.3}$$

It can be seen that for some parameter domains the dependence (2.3) is given by the graph, such that the tangent line to it at $k=0$ doesn't intersect it any more and bifurcation occurs from zero wave number. In this case we have ordinary solitary waves in the weakly nonlinear limit given by Korteweg-de Vries (KdV) solitons. For the certain parameter domain (to be specified below) we have bifurcations at finite wave number – the place on the dispersion curve $\omega=\omega(k)$ where the line $\omega/k=V_0$ (V_0 is the critical value of the wave velocity) is tangent to it at the finite wave number k (the phase speed ω/k is equal to the group speed $d\omega/dk$). In the latter case one has envelope solitary waves in the weakly nonlinear limit given by nonlinear Schrödinger (NLS) solitons. The sketches of graphs of the dependence (2.3) $\omega=\omega(k)$ for these two cases is shown in Fig. 1. Moreover, presumably we have in our model non-stationary envelope solitary waves whose phase and group velocities are not equal (we do not consider them here).

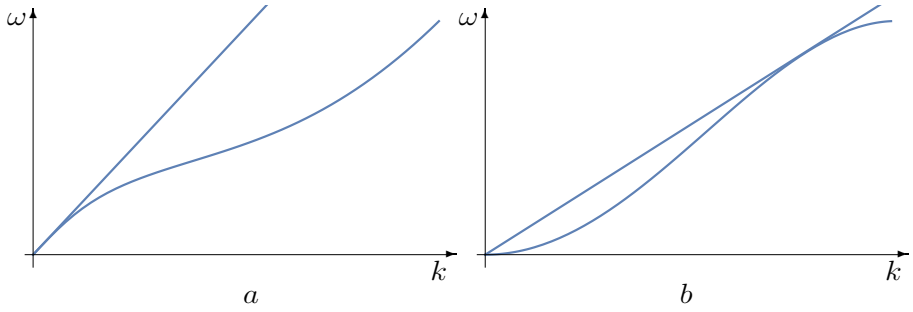

Figure 1: Bifurcation from zero wave number leading to KdV-type solitary waves (a); bifurcation at finite wave number leading to NLS-type solitary waves (b)

3 Traveling waves

Consider a traveling wave which propagates to the left with the velocity V along the x-axis. In the coordinates moving with the speed V the components of the velocity vector of particles $\mathbf{v}=(u,v)^\top$ satisfy the following asymptotic conditions $u\to V$, $v\to 0$, $x\to\infty$.

Make, further, the following scaling transformations:

$$(x,z)\to\left(\frac{x}{H},\frac{z}{H}\right),\quad \eta\to\frac{\eta}{H},\quad \mathbf{v}\to\frac{\mathbf{v}}{V}.$$

For these transformations $D \to \Omega$, $\partial D^{\pm} \to \partial\Omega^{\pm}$,

$$\Omega = \{x \in \mathbb{R};\ 0 < z < 1 + \eta(x)\}, \quad \partial\Omega = \partial\Omega^{+} \cup \partial\Omega^{-} = \{x \in \mathbb{R}; z = 1 + \eta(x) \cup z = 0\}.$$

In new dimensionless variables (for them we use the previous notations) the Euler equations (2.2) for traveling waves have the form

$$\begin{aligned}
&\operatorname{rot}\mathbf{v} = \mathbf{0}, \quad \operatorname{div}\mathbf{v} = 0, \qquad (x,z) \in \Omega;\\
&\frac{1}{2}|\mathbf{v}|^2 + \lambda\eta - b\kappa_1 + \gamma\kappa_2 + c(\partial_{xx}\eta - \kappa_1) = \text{const}, \qquad (x,z) \in \partial\Omega^{+};\\
&\partial_x\eta\, u - v = 0, \qquad (x,z) \in \partial\Omega^{+};\\
&v = 0, \qquad (x,z) \in \partial\Omega^{-}.
\end{aligned} \tag{3.1}$$

The constants λ, b, γ, c κ are determined by

$$\lambda = gH/V^2, \quad b = \frac{\hat{b}}{HV^2} - c, \quad \gamma = \frac{J}{\rho V^2 H^3}, \quad c = \frac{\hat{c}}{H}, \quad \kappa = \frac{h}{H}. \tag{3.2}$$

The functions κ_j, $j = 1, 2$, are given by

$$\kappa_1 = \frac{\partial_{xx}\eta}{(1 + (\partial_x\eta)^2)^{3/2} - \kappa\partial_{xx}\eta}, \qquad \kappa_2 = \partial_{xx}^2 \frac{\partial_{xx}\eta}{(1 + (\partial_x\eta)^2)^{3/2} - \kappa\partial_{xx}\eta}.$$

It can be shown that Eqs. (3.1) can be written locally in the operator form

$$\partial_x \mathbf{u} = \mathcal{A}(\boldsymbol{\lambda})\mathbf{u} + \mathbf{G}(\boldsymbol{\lambda}, c, \mathbf{u}). \tag{3.3}$$

where $\boldsymbol{\lambda} = (\lambda, b, \gamma)^{\top}$, the vector function $\mathbf{u}$ is the unknown, $\mathcal{A}(\boldsymbol{\lambda})$ is the linear closed unbounded operator acting in certain functional spaces, $\mathbf{G}(\boldsymbol{\lambda}, c, \mathbf{u})$ is the nonlinearity, μ is a small constant [11].

Bifurcations from the quiescent state giving rise to the appearance of non-trivial bounded wave patters occur when eigenvalues of the operator $\mathcal{A}$ come to the imaginary axis. This takes place in the following two cases (see Fig. 2)

• On the plane $\lambda = \lambda_0 = 1$, $b = b_0 \neq 1/3$ and $\gamma = \gamma_0 \in \mathbb{R}^+/0$ in the λ, b, γ parameter space. For $\lambda > 1$, $\beta > 1/3$ and $\gamma > 0$ we get, in particular, the interface between the water and ice plate in the form of solitary wave of depression (corresponds to the case shown in Fig. 1a); for $\lambda < 1$, $b < 1/3$ and $\gamma > 0$ we get, in particular, the interface between the water and ice plate in the form of generalized solitary wave of elevation with non-decaying periodic asymptotic at infinity [6].

• In the neighborhood of the surface in the parameter (λ, b, γ) space, parameterized by $\{q, \gamma_0\}$, where q is the dimensionless wave number $q = kH$ (wave length $l = 2\pi/k$) and given by

$$\begin{aligned}
\lambda_0 &= \gamma_0 q^4 + \frac{q\coth q}{2} + \frac{q^2\sinh^{-2} q}{2} \equiv f(\gamma_0, q),\\
b_0 &= -2\gamma_0 q^2 + \frac{\coth q}{2q} - \frac{\sinh^{-2} q}{2} \equiv e(\gamma_0, q),
\end{aligned} \tag{3.4}$$

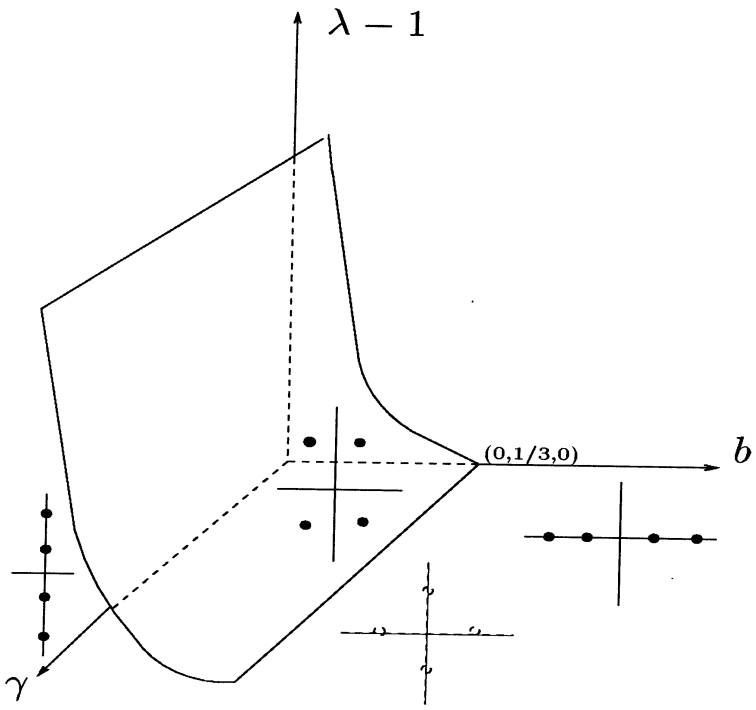

Figure 2: The surfaces $\lambda = 1$ and (3.4), where the bifurcation in the parameter (λ, b, γ)-space occurs. Locations of the eigenvalues coming in pairs to the imaginary axis on these surfaces are indicated by black circles on both sides of the surface (3.4) and over the plane $\lambda = 1$, and by white circles under the plane $\lambda = 1$

the bifurcation from the quiscent state takes place leading to the appearance of envelope solitary waves (corresponds to the case shown in Fig. 1b) or dark solitons [6].

The parameter of bifurcation $|\mu| \ll 1$ is chosen so that

$$\lambda = \lambda_0 + \mu. \tag{3.5}$$

The bifurcation parameter is the wave velocity V. From (3.5) it follows that

$$V^{-2} = V_0^{-2} + \frac{\mu}{gH}$$

and

$$b = b_0 + \omega_1\mu, \quad \gamma = \gamma_0 + \omega_2\mu, \quad \mu \ll 1, \quad \omega_1 = \frac{h\sigma_0}{\rho g H^2}\mu, \quad \omega_2 = \frac{J}{\rho g H^4}. \tag{3.6}$$

Further, we will consider (3.3) in a neighborhood of the surface (3.4), defined by (3.5), (3.6). Denote

$$\mathcal{A} = \mathcal{A}(\boldsymbol{\lambda}_0), \quad \mathbf{F}(\mu, \mathbf{u}) = \mathbf{G}(\lambda_0 + \mu, b_0 + \frac{h\sigma_0}{\rho g H^2}\mu, \gamma_0 + \frac{J}{\rho g H^4}\mu, c, \mathbf{u}).$$

Then (3.3) can be rewritten as

$$\dot{\mathbf{u}} = \mathcal{A}\mathbf{u} + \mathbf{F}(\mu, \mathbf{u}), \qquad \mathcal{A} = \mathcal{A}(\boldsymbol{\lambda}_0), \quad \mathbf{F}(0, \mathbf{0}) = 0, \quad \partial_{\mathbf{u}}\mathbf{F}(0, \mathbf{0}) = 0, \tag{3.7}$$

where the upper dot denotes the differentiation with respect to the unbounded coordinate x.

4 Centre manifold reduction and normal form approximation

Hereinafter we briefly indicate how Eqs. (3.1) written in the form (3.7) can be solved to obtain the envelope solitary wave solutions. To do this we need to complete the following three steps.
Step 1. Projection to the centre manifold. We project our system of partial differential equations to the subspace of infinite dimensional phase space of the system in question where the bounded small amplitude solutions of it live. This subspace has the same dimension as the space spanned by the null eigenvectors of the operator $\mathcal{A}$. Since the number of the null eigenvalues of $\mathcal{A}$ is finite (in our case their number is four) the phase space of the resulting system is finite dimensional (four dimensional) and we get the flow on the centre manifold given by the ordinary differential equation of the fourth order. We formulate the corresponding theorem (Theorem 1) in Subsec. 4.1
Step 2. Approximation by the normal form system. The flow on the centre manifold, given by the reduced ordinary differential system of the fourth order is approximated by the system in the normal form up to an arbitrary algebraic order with respect to μ. The resulting normal form system appears to be integrable (Theorem 2 below).
Step 3. Persistence of envelope solitary wave solutions. It can be proved that there exist the envelope solitary wave solution to full system (3.1) [26]. Moreover, the envelope solitary wave solution to the cut-off normal form equations approximates to the corresponding order the envelope solitary wave solution to (3.1), when their amplitudes are small enough (Theorem 3 below).

4.1 Centre manifold reduction

In the case in question the following results are valid (see [11] and references therein).

Theorem 1 (about centre manifold, [5]). *The manifold*

$$M_\mu = \big\{\big(\mathbf{u}_0, \mathbf{h}(\mu, \mathbf{u}_0)\big) \in X, \quad ||\mathbf{u}_0|| < \varepsilon\big\}, \quad \varepsilon \ll 1, \quad \mathbf{u}_0 \in X_0,$$

($||\cdot||$*denotes a norm in* X) *is the invariant manifold of the dynamic system* (3.7)*, contains all small bounded solutions of this system and is called the centre manifold. The dimension of the space* X_0 *is finite, that is equivalent to finiteness of number of the imaginary*

eigenvalues (with their multiplicity) of the operator $\mathcal{A}$. The system of equations (3.7) *after projection on the space X_0 and its complementary one in X (denoted further as X_1) takes the form*

$$\begin{aligned}\dot{\mathbf{u}}_0 &= \mathcal{A}_0\mathbf{u}_0 + \mathbf{F}_0(\mu, \mathbf{u}_0 + \mathbf{u}_1),\\ \dot{\mathbf{u}}_1 &= \mathcal{A}_1\mathbf{u}_1 + \mathbf{F}_1(\mu, \mathbf{u}_0 + \mathbf{u}_1),\end{aligned} \tag{4.1}$$

where

$$\mathbf{u} = (\mathbf{u}_0, \mathbf{u}_1)^\top \in X = X_0 \times X_1, \quad \mathcal{A}_0 = \mathcal{A}|_{X_0}, \quad \mathcal{A}_1 = \mathcal{A}|_{X_1 \cap D(\mathcal{A})},$$

and $\mathbf{F}_j$, $j = 0, 1$ are the projections of $\mathbf{F}$ on X_0 and X_1, correspondingly. Besides,

- $\mathbf{h}(0, \mathbf{0}) = \partial_{\mathbf{u}_0}\mathbf{h}(0, \mathbf{0}) = \mathbf{0}$;
- *if $\mathcal{R} = \mathcal{R}_0 \oplus \mathcal{R}_1$, $\mathcal{R}_0 : X_0 \to X_0$, $\mathcal{R}_1 : X_1 \to X_1$ are linear isometries, such that $\mathbf{F}_j(\mu, \mathcal{R}_0\mathbf{u}_0, \mathcal{R}_1\mathbf{u}_1) = -\mathcal{R}_j\mathbf{F}_j(\mu, \mathbf{u}_0, \mathbf{u}_1)$, $\mathcal{A}_j\mathcal{R}_j = -\mathcal{R}_j\mathcal{A}_j$, $j = 0, 1$, then $\mathbf{h}(\mu, \mathcal{R}_0\mathbf{u}_0) = \mathcal{R}_1\mathbf{h}(\mu, \mathbf{u}_0)$.*

The assertions of Theorem 1 mean, that until the inequality $||\mathbf{u}_0|| < \varepsilon$ is valid, the solution $\mathbf{u} = (\mathbf{u}_0, \mathbf{u}_1)^\top$ of (4.1) belongs to M_μ, i. e. $\mathbf{u}_1 = \mathbf{h}(\mu, \mathbf{u}_0)$. Consequently, the set of all small bounded solutions obeys the finite dimensional dynamic system of equations:

$$\dot{\mathbf{u}}_0 = \mathcal{A}_0\mathbf{u}_0 + \mathbf{f}_0(\mu, \mathbf{u}_0), \;\; \mathbf{f}_0(\mu, \mathbf{u}_0) = \mathbf{F}_0(\mu, \mathbf{u}_0 + \mathbf{h}(\mu, \mathbf{u}_0)). \tag{4.2}$$

The equations (4.2) are called the reduced equations.

4.2 Normal form approximation

It can be shown, that for the case in question $\mathbf{u}_0 = \big(A, B, A^*, B^*\big)^\top$, and the following theorem is valid.

Theorem 2 [26]. *The reduced equations* (4.2) *are approximated by the system in the normal form*

$$\begin{aligned}\partial_x A &= iqA + B + iAR\Big(AA^*, \frac{i}{2}(AB^* - A^*B)\Big),\\ \partial_x B &= iqB + AQ\Big(AA^*, \frac{i}{2}(AB^* - A^*B)\Big) + iBR\Big(AA^*, \frac{i}{2}(AB^* - A^*B)\Big)\end{aligned} \tag{4.3}$$

up to arbitrary algebraic order with respect to μ. Here R and Q are polynomials with real coefficients:

$$\begin{aligned}R(\mu, u, K_0) &= p_1\mu + p_2 u + p_3 K_0 + O\big((|\mu| + |u| + |K_0|)^2\big),\\ Q(\mu, u, K_0) &= q_1\mu - q_2 u + q_3 K_0 + O\big((|\mu| + |u| + |K_0|)^2\big).\end{aligned}$$

Under the action of the isometry $\mathcal{R}_0$, $A \to A^*$, $B \to -B^*$. *The system of equations* (4.3) *has two first integrals*

$$K_0 = \frac{i}{2}(AB^* - A^*B), \quad H_0 = |B|^2 - S(\mu, |A|^2, K_0), \quad S = \int_0^{|A|^2} Q(\mu, u, K_0)\, du,$$

and, consequently, appears to be the integrable one.

It can be shown with the help of (4.3) [26] that the reduced system (4.2) has solitary wave solutions with equal phase and group speeds; the interface deviation is given by [26]

$$\eta = 1 \pm \frac{2\tanh q}{q^2}\sqrt{\frac{2\mu q_1}{q_2}}\cosh^{-1}\sqrt{\mu q_1}x\cos qx + O(|\mu|^{3/2}), \tag{4.4}$$

where the constants q_1 and q_2 depends on q. The constant $q_1 > 0$ for all q, the constant q_2 changes sign. If $q_2 > 0$ (4.4) gives the envelope solitary wave for $\mu > 0$ (see Fig. 3).

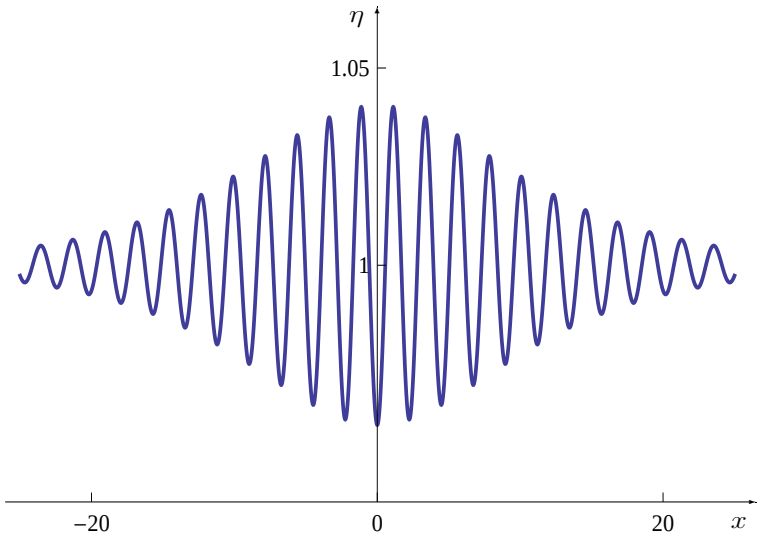

Figure 3: Form of the interface between the water and the ice given by an envelope solitary waves of depression (4.4) for $H = 55$ m, $h = 1$ m, $\sigma_0 = 10^5$ Nm^{-1} and $\mu = 0.005$; E=5$\times$ 10^9 N·m^{-2} and $\nu = 0.3$, $\rho = 1000$ kg·m^{-3}, $g = 10$ m·s^{-1}

If $q_2 < 0$, $\mu < 0$ we get the so-called dark soliton

$$\eta = 1 \pm \frac{2\tanh q}{q^2}\sqrt{\frac{\mu q_1}{q_2}}\tanh\sqrt{\frac{-\mu q_1}{2}}x\sin qx + O(|\mu|^{3/2}). \tag{4.5}$$

The dark soliton is the nonlinear product of the periodic wave and the bore for $q_2 < 0$, $\mu < 0$ (see Fig. 4).

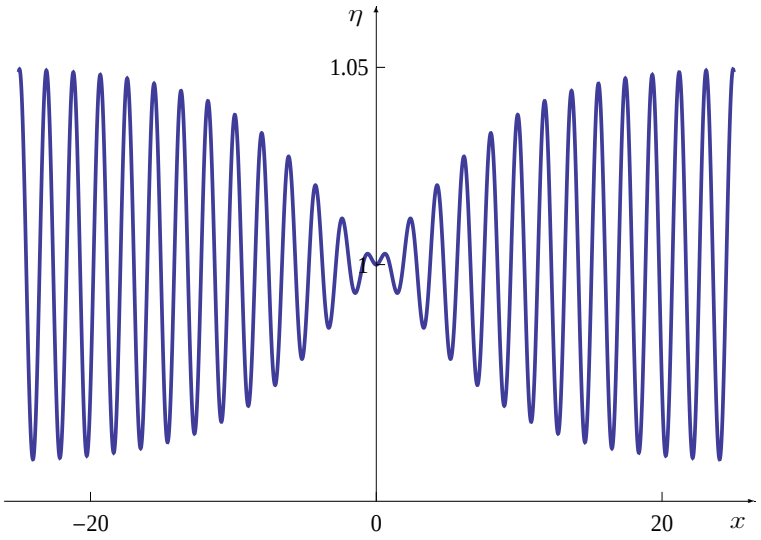

Figure 4: Form of the interface between the water and the ice given by a dark soliton of elevation (4.5) for $H = 65$ m, $h = 1$ m, $\sigma_0 = 10^5$ Nm^{-1} and $\mu = -0.005$. The other parameters are as in Fig. 3

Because the function $q_2(q)$ changes the sign for finite q there exists critical depths H_c where envelope solitary waves are replaced by dark solitons [12]. The solution (4.4) corresponds to the vector-function $\mathbf{u}^r_{0s} = \left(A^r_s, B^r_s, A^{r*}_s, B^{r*}_s\right)^\top$.

Theorem 3 [26]. *There exists the family of envelope solitary waves* $\mathbf{u}_{0s} = (A_s, B_s, A^*_s\, B^*_s)^\top$, *satisfying the reduced equations* (4.2). *Besides, the mentioned solutions of the reduced equations differ little from* $\mathbf{u}^r_{0s}$, *exactly* :

$$|\mathbf{u}_{0s} - \mathbf{u}^r_{0s}| \leq \tilde{c}\mu\, \exp(-\chi\sqrt{\tilde{\mu}}x),$$

where $\tilde{\mu} = q_1\mu > 0$, $\tilde{c} > 0$ *is some constant, and* $0 < \chi < 1$.

5 Results

Usually inertia of the ice plate is small in comparison with that of the water layer and it produces a weak effect on physical parameters of the phenomena (see, e. g. [12]). Therefore, we put c and κ to zero. The constants q_1 and q_2 can be computed directly [27] and in this case are given by the following expressions.

$$q_1 = \frac{1 + \omega_1 q^2 + \omega_2 q^4}{(2b_0 q + 4\gamma_0 q^3)\coth q + 6\gamma_0 q^2 + b_0 - 1} > 0, \tag{5.1}$$

$$q_2 = -\frac{r}{16q^4(\lambda_0-1)\cosh^3 q}\big(\lambda_0 - 9{\lambda_0}^2 + 16q^2 - 12\lambda_0\cosh 2q + +12{\lambda_0}^2\cosh 2q +$$
$$+11\lambda_0\cosh 4q - 3{\lambda_0}^2\cosh 4q + 14q\sinh 2q + 16\alpha q\sinh 2q + 18\hat{\lambda}q\,\mathrm{sh}\,2q -$$
$$-16\alpha\lambda_0 q\sinh 2q + q\sinh 4q + 4\alpha q\sinh 4q - \lambda_0 q\sinh 4q - 4\alpha\lambda_0 q\sinh 4q\big),$$
$$r = \frac{q^4\coth q}{\lambda_0 q\cosh q - b_0 q^3\cosh q - 3\gamma_0 q^5\cosh q - \lambda_0\sinh q - 3\gamma_0 q^4\sinh q},$$
$$\alpha = \frac{2(2+\cosh 2q)}{-5-\cosh 2q + 6q\coth q - 18\gamma_0\, q^3\sinh 2q}. \tag{5.2}$$

From (3.2) and (3.4) one has

$$e(\gamma_0, q) - \frac{h\sigma_0}{\rho g H^2} f(\gamma_0, q) = 0,$$
$$\gamma_0 - \frac{J}{\rho g H^4} f(\gamma_0, q) = 0. \tag{5.3}$$

From (5.3) we have

$$\gamma_0 = \frac{(\rho g H^2 - h\sigma_0 q^2)\coth q - q(\rho g H^2 + h\sigma_0 q^2)\sinh^{-2} q}{4\rho g H^2 q^3 + 2h\sigma_0 q^5}, \tag{5.4}$$

where $q = q_0$ is a root of the equation

$$(3Jq^4 - \rho g H^4 + hH^2\sigma_0 q^2)\cosh q + q(Jq^4 + \rho g H^4 + hH^2\sigma_0 q^2)\sinh^{-1} q = 0. \tag{5.5}$$

The case when the ice plate is subjected to the compression was discussed in [13]. Possible compression pre-stresses σ_0 (admissible tensions) which provide the stability of the quiescent states were computed there in dependence on the thickness of the ice plate. In Table 2 we give the corresponding values of physical parameters for the initially stressed ice plate. In the case of compression the value of σ_0 is negative. The form of the envelope solitary wave given by for $\sigma_0 = 10^5$ N·m^{-2} is shown in Fig. 3

σ_0 Nm^{-2}	V_0 m s^{-1}	$l = 2\pi H/q_0$ m	q_0	γ_0	λ_0	b_0
10^6	17.44	132.01	2.6	0.009	1.81	0.066
10^5	16.12	123.95	2.8	0.011	2.12	0.007
0	15.95	122.59	2.82	0.011	2.15	0
-10^5	15.35	121.68	2.84	0.011	2.2	−0.007
-10^6	14.28	114.05	3.03	0.013	3.03	−0.09

Table 2: Dimensional pre-tension in ice cover, characteristic values of speed and length of envelope solitary wave and non-dimensional parameters for $H = 55$ m and $h = 1$ m.

The constants q_1 and q_2 in (4.4) are given by (5.1) and (5.2) where γ_0 is given by (5.4). To establish the dependence of q_2 on H the following steps have to be undertaken.

• First, (5.4), (3.4) and (3.5) have to be substituted in (5.1) and (5.2).

• Second, from (5.5) we obtain the dependence $q(H)$ and substitute it in (5.2). The example of the dependence $q_2(H)$ is illustrated by Fig. 5.

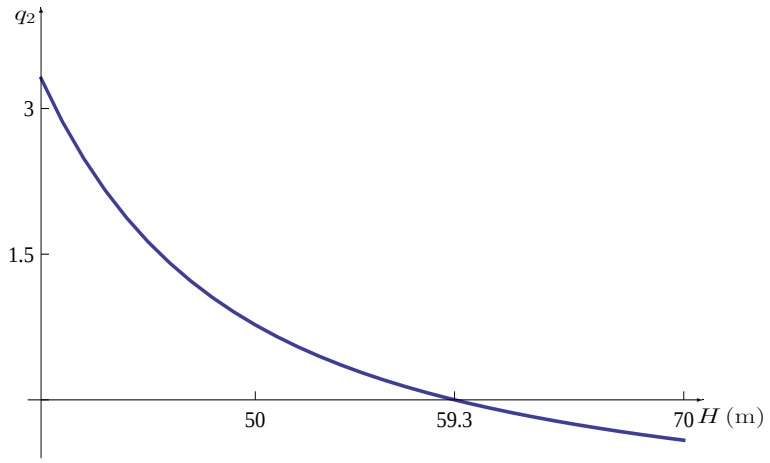

Figure 5: Dependence of q_2 on H for $\sigma_0 = 10^5$ N·m^{-2}. The other physical constants are as in Fig. 3

6 Conclusion and discussion

The result of the present research is an attempt to build bridges between theoretical predictions and results of measurements of waves characteristics beneath the ice, which are made, in particular, at the Institute of Arctic and Antarctic in St. Petersburg, Russia. **The main aim of our investigation is to put in an explicit form the procedure of computing physical parameters of the envelope solitary wave (the wave length, wave velocity, etc.). Of course, envelope solitary waves on the water surface under the ice cover have been studied in many papers, but, to our knowledge, the general correspondence of their theoretical description to possible experimental detection in the naturel water basins is evaluated for the first time in this paper. For this purpose we use the theoretical expression for the envelope solitary wave, that are known to exist in the model to be briefly specified below.**

For theoretical description we use the full 2D Euler equations. The Euler equations involve the additional pressure from the plate that is freely floating at the surface of the fluid. The ice cover is modeled by an elastic Kirchhoff-Love plate and is assumed to be of considerable thickness so that the inertia of the plate is taken into account in the formulation of the model. The plate itself is physically linear (Hooke's law is valid), but geometrically nonlinear. Consequently, we are able to treat finite (not small) displacements, though we are restricted to small strains. We consider the self-focusing case, when due to Theorem 3 envelope solitary waves exist , for which the envelope velocity (group velocity) is equal to the velocity of filling (phase velocity). Analysing envelope solitary waves ($q_2 > 0$, $\mu > 0$) for all possible values of parameters we are able to find theoretical values for corresponding wave length and wave velocity. In particular, it is established that envelope solitary waves are long waves propagating with a considerably high speed. The example of

corresponding parameters for specific depth and ice thickness values are given in Table 2. As follows from the results of the paper [18], where the ice sheet model is based on the special Cosserat theory, the small- to large amplitude envelope solitary waves of depression are stable. We assume that this is true also for the plate model of the ice sheet used here. Therefore, in Fig. 3 we give the graph of the form of the wave of depression of the small amplitude.

The self-focusing takes place for the water depths $H < H_c(h)$, the coefficient at the leading nonlinearity $q_2(H_c) = 0$ and changes in this point its sign for any given ice thickness h. When $H > H_c(h)$ the envelope solitary wave is replaced by the dark soliton, which is the indicator of modulational stability [12]. It can be seen from Fig. 5 that for physically reliable initial tensions $\sigma_0 = 10^5$ N m^{-2} and the ice thickness $h = 1$ m the critical value $H_c \approx 59.3$ meters.

For the case of small amplitudes (small μ, though dimensional values can reach several tens of centimeters) treated here the typical values of parameters (wave velocity and wave length) are evidently close to those given by Table 2 (in case of the corresponding water depth and ice thickness). Due to high value of the Young module of the ice it is not visible how the waves of large amplitude can appear in practice. Therefore, it is natural to compare theoretical values of the wave velocity and length of envelope solitary waves evaluated here with those given by natural observations of these wave structures in natural basins. The detection of envelope solitary waves under the ice cover may be based on corresponding measurements of their velocity. Then, **one can measure the wave amplitude and, therefore,** compute the parameter μ, corresponding to an experimental value of the wave amplitude. Next, we compare theoretical and experimental values of the wave length. A follows from (4.4) the length of the envelope depends on μ and the length of the filling is given by the dimensionless wave number q, which for given parameters H, h and σ_0 is determined from (5.5).

References

[1] L.K. Forbes, Surface waves of large amplitude beneath an elastic sheet. High order series solution, *J. Fluid Mech.* 1986. **169**. 409–428.

[2] L.K. Forbes, Surface waves of large amplitude beneath an elastic sheet. Galerkin solutions, *J. Fluid Mech.* 1988. **188**. 491–508.

[3] G. Iooss, M. Adelmeyer, *Topics in Bifurcation Theory and Applications*. World Scientific, 1992.

[4] K. Kirchgässner, Wave solutions of reversible systems and applications, *J. Diff. Eqns.* 1982. **45**. 113–127.

[5] A. Mielke, Reduction of quasilinear elliptic equations in cylindrical domains with applications, *Math. Meth. Appl. Sci.*. 1988. **10**. 501–566.

[6] A. Il'ichev, Solitary waves in media with dispersion and dissipation (a review), *Fluid Dyn.* 2000. **35**. 157–176.

[7] E. Parau, F. Dias, Nonlinear effects in the response of a floating ice plate to a moving load, *J. Fluid Mech.* 2002. **460**. 281–305.

[8] P. A. Milewskii, J.-M. Vanden-Broeck and Z. Wang, Hydroelastic solitary waves in deep water, *J. Fluid Mech.* 2011. **679**. 628-640.

[9] J.-M. Vanden-Broeck, E. Părău, Two dimensional generalized solitary waves and periodic waves under an ice sheet, *Phil. Trans. R. Soc. Lond.* 2011. **A369**. 2957–2972.

[10] E. Părău, J.-M. Vanden-Broeck, Three dimensional waves beneath an ice sheet due to a steadily moving pressure, *Phil. Trans. R. Soc. Lond.* 2011. **A369**. 2973–2988.

[11] A.T. Il'ichev, Soliton-like structures on a water-ice interface, *Russian Math. Surveys.* 2015. **70**. 1051-1103.

[12] A.T. Il'ichev, Envelope solitary waves and dark solitons at a water-ice interface, *Proc. Steklov Inst. Math.* 2015. **289**. 152-166.

[13] A. T. Il'ichev, Solitary wave packets beneath a compressed ice cover, *Fluid Dyn.* 2016. **51**. 327-337.

[14] P.I.Plotnikov, J.F.Toland, Modelling nonlinear hydroelastic waves, *Phil. Trans.the R. Soc. A.* 2011. **369**. 2942-2956.

[15] A. Müller, R. Ettema, Dynamic response of an icebreaker hull to ice breaking, *Proceedings of the 7th IAHR International Symposium on Ice.* 1984. **II**. Hamburg, W. Germany. 287-296.

[16] P. Guyenne, E.I. Părău, Computations of fully nonlinear hydroelastic solitary waves on deep water, *J. Fluid Mech.* 2012. **713**. 307–329.

[17] Z. Wang, J-M.Vanden-Boeck, P.A. Milevski, Two dimensional flexural-gravity waves waves of finite amplitude in deep water, *IMA J. Appl. Math.* 2013. **78**. 750–761.

[18] P. Guyenne, E.I. Părău, Finite-depth effects on solitary waves in a floating ice sheet, *Journal of Fluids Structures.* 2014. **49**. 242-262.

[19] Z. Wang, E. I. Părău, P.A. Milewski, J-M. Vanden-Broeck, Numerical study of interfacial solitary waves propagating under an elastic sheet, *Proc. R. Soc. A.* 2014. **470**: 20140111.

[20] E. I. Părău, **Solitary** interfacial hydroelasic waves, *Phil. Trans. R. Soc. A.* 2017. **376**: 20170099.

[21] T. Gao, J.-M. Vanden-Broeck, Z. Wang, Numerical computations of two-dimensional flexural-gravity solitary waves on water of arbitrary depth, IMA J. Applied Math, to appear.

[22] O. Trichtchenko, E. I. Părău, J.-M. Vanden-Broeck, P. A. Milewskii, Solitary flexuralgravity waves in three dimensions, *Phil. Trans. R. Soc. A*. 2018. **376**:20170345.

[23] T. Takizava, Responce of a floating sea ice sheet to a steadily moving load, *J. Geophys. Res.*, 1988. **93**. 5100–5112.

[24] V. A. Squire, W. H. Robinson, H. J. Langhorne, N. G. Haskell, Vehicles and aircraft on floating ice. *Nature*. 1988. **333**. 159–161.

[25] J. R. Marko, Obserations and analyses of an intense waves-in-ice event in the Sea of Okhotsk, *J. Geophys. Res.* 2003. **108**. 3296.

[26] G. Iooss , M. C. Perouéme, Perturbed homoclinic solutions in reversible 1:1 resonance vector fields, *J. Diff. Eqns*. 1993. **102**. 62–88.

[27] F. Dias, G. Iooss, Capillary-gravity solitary waves with damped oscillations, *Physica D*. 1993. **65**. 399–423.